SNR Enhancement Algorithm Using Multiple Chirp Symbols with Clock Drift for Accurate Ranging

Seong-Hyun Jang, Yeong-Sam Kim, Sang-Hun Yoon, and Jong-Wha Chong

A signal-to-noise ratio (SNR) enhancement algorithm using multiple chirp symbols with clock drift is proposed for accurate ranging. Improvement of the ranging performance can be achieved by using the multiple chirp symbols according to Cramer-Rao lower bound; however, distortion caused by clock drift is inevitable practically. The distortion induced by the clock drift is approximated as a linear phase term, caused by carrier frequency offset, sampling time offset, and symbol time offset. SNR of the averaged chirp symbol obtained from the proposed algorithm based on the phase derotation and the symbol averaging is enhanced. Hence, the ranging performance is improved. The mathematical analysis of the SNR enhancement agrees with the simulations.

Keywords: Multiple chirp symbols, SNR enhancement, clock drift, ranging, linear phase.

Seong-Hyun Jang (phone: +82 2 2220 0558, email: zeusjang@gmail.com), Yeong-Sam Kim (email: ys31205@hanyang.ac.kr), and Jong-Wha Chong (email: jchong@hanyang.ac.kr) are with the Department of Electronics and Computer Engineering, Hanyang University, Seoul, Rep. of Korea.

Sang-Hun Yoon (corresponding author, email: shyoon11@etri.re.kr) is with the Convergence Components & Materials Research Laboratory, ETRI, Daejeon, Rep. of Korea.

I. Introduction

For decades, chirp has been widely used for localization with time delay estimation (TDE) methods. Chirp has an excellent ability to decompose multipath into individual path due to its good correlation property as in [1]. In TDE, Fourier transform, which is essential to obtain channel frequency response, imposes additional complexity. However, chirp helps us to reduce additional complexity by using a dechirping process in [2] because the complexity of dechirping process is much smaller than that of Fourier transform. Especially, the TDE problem of the linear chirp can be converted into the frequency estimation problem of the sinusoid through the dechirping process in [2]. Thus, the linear chirp can be applied to the estimation of signal parameters via rotational invariance techniques (ESPRIT) in [3], which is one of frequency estimation algorithms based on the subspace separation.

Generally, precise localization depends on the ranging precision between nodes. Increment of signal-to-noise ratio (SNR) or bandwidth is necessary to improve the precision of the ranging method based on TDE according to Cramer-Rao lower bound as in [4]. Alternatively, the ranging precision can also be improved by using multiple symbols without violating Federal Communications Commission regulations because increment of SNR can be achieved through the average of the multiple symbols.

When multiple symbols are transmitted, additive noise is averaged out if received multiple symbols are coherently added for the averaged chirp symbol. In other words, the effect of extension of observation time is converted into that of enhancement of SNR of averaged symbol through the symbol averaging. Generally, symbol averaging denotes the averaging of the multiple symbols as in [5]. However, as observation time

is extended in practical systems, clock drift occurs from the mismatch between local oscillators of the transmitter and the receiver. The clock drift generates carrier frequency offset in frequency. Moreover, the sampling time offset and symbol time offset are also produced in time. As a result, multiple symbols are distorted. The distortion is modeled as a linear phase variation which consists of carrier frequency offset, sampling time offset, and symbol time offset. The linear phase variation can be eliminated by phase derotation. The phase derotation is   compensation by multiplying the conjugate of the linear phase variation as in [6]. As a result, additive noise cannot be averaged out by the symbol averaging as long as the clock drift exists; therefore, the clock drift disturbs the enhancement of SNR.

Many studies have been conducted in order to reduce the distortion of the clock drift for ranging system in [7]-[9]. Some research aims for ultra wideband ranging system in [7], [8] where those algorithms are not applicable to the ranging system using narrowband signals. In [9], symmetric double side-two way ranging (SDS-TWR) has been proposed to remove the sampling time offset caused by the clock drift through the average of two TWR estimates. Although SDS-TWR is one of the solutions to the problem caused by the clock drift, it does not consider carrier frequency offset (CFO) caused by the clock drift. Besides, the SDS-TWR is a postprocessing method, that is, the distortion caused by clock drift is reduced after TDE is accomplished; so, it cannot be employed to the ranging system using multiple symbols. Therefore, SDS-TWR cannot eliminate the distortion induced of clock drift inherent in multiple symbols completely. Even in the ranging system based on the subspace separation in [10], the clock drift is ignored.

Therefore, it is indispensable to develop the algorithm that alleviates the distortion caused by clock drift before TDE and that enhances SNR of the averaged chirp symbol in the localization systems using multiple chirp symbols for accurate ranging.

II. Signal Models

A linear chirp symbol can be defined as

$$s(t) = \exp\left(\frac{j\pi\beta t^2}{T_{\text{sym}}}\right), \quad |t| < \left(\frac{T_{\text{sym}}}{2} - T_{\text{guard}}\right), \quad (1)$$

where β is a total bandwidth during the symbol duration T_{sym}. When β is positive, the chirp is an up-chirp; if β is negative, it is a down-chirp. T_{guard} is guard time which is enough large to ignore inter-symbol interference between adjacent symbols. For the convenience of mathematical analysis, the center

frequency of chirp symbol is assumed to be zero. Adopting a tapped-delay-line multipath channel model, the received chirp corrupted by multipath channel and CFO induced by clock drift can be modeled as

$$r(t) = e^{j(\omega_{\text{CFO}} t + \varphi)}\sqrt{E_s}\sum_{m=1}^{M}\sum_{k=1}^{K}\alpha_k e^{jc_m}s(t - \tau_k - mT_{\text{sym}}) + g(t), (2)$$

where ω_{CFO} ($=\delta\omega_c$) is CFO and φ is initial phase. Let δ be the clock drift. E_s represents average energy of the received signal and M denotes the total number of chirp symbols. K is the number of received multipath components with α_k and τ_k denoting the complex amplitude and delay of the k-th path, respectively. The complex amplitudes of the multipath are normalized, that is, $\sum_{k=1}^{K}E[|\alpha_k|^2] = 1$. $E[\cdot]$ represents the expectation. It is assumed that the channel is invariant during the transmission of multiple symbols. c_m is a modulated phase of the m-th symbol. Because c_m can be estimated and compensated by using signal detector, it is assumed that c_m is zero afterwards. Here, $g(t)$ is additive white Gaussian noise (AWGN) with variance σ^2.

III. Problem Definition

In order to increase the SNR for accurate ranging, multiple chirp symbols are employed. It is reasonable to consider the sampling time offset and the symbol time offset which are induced by clock drift because multiple chirp symbols are concatenated. Then, after sampling of the received multiple chirp symbols in (2), the received n-th sample in the m-th chirp symbol can be modeled as

$$
\begin{aligned}
r(n, m) &= \left(e^{j\left(\omega_{\text{CFO}}\left(n(T_s - \varepsilon) + m(T_{\text{sym}} - \kappa)\right) + \varphi\right)}\right. \\
&\quad \left. \times \sqrt{E_s}\sum_{k=1}^{K}\alpha_k s\left(n(T_s - \varepsilon) - \tau_k - m\kappa\right)\right) + g(n, m) \\
&= x(n, m) + g(n, m),
\end{aligned}
\quad (3)
$$

where n and m are the sample index ($n=1,\ldots,N$) and the symbol index ($m=1,\ldots, M$), respectively, and T_s is sampling interval. Then, sampling time offset in a symbol duration is denoted as $\varepsilon = (T_s-(T_s/(1+\delta))) = (\delta T_s/(1+\delta)) \approx \delta T_s$. Symbol time offset is represented as $\kappa = \varepsilon(T_{\text{sym}}/T_s) \approx \delta T_{\text{sym}}$. N is the total number of samples, and M is the total number of chirp symbols. In (3), $g(n, m)$ are complex zero mean Gaussian random variables with variance σ^2.

Symbol averaging is represented as

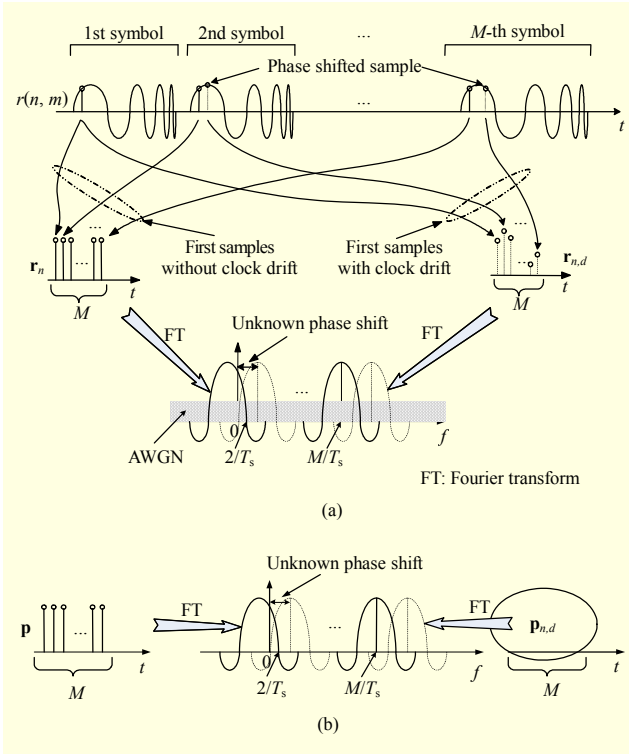$$r_{\text{avg}}(n) = \frac{1}{M}\sum_{m=1}^{M}r(n, m) = (\mathbf{r}_n)^T \mathbf{p}, \quad (4)$$

Fig. 1. Effect of clock drift on received samples in frequency domain: (a) frequency responses of two sets $\mathbf{r}_n$: first samples of multiple symbols without clock drift and $\mathbf{r}_{n,d}$: first samples of multiple symbols with clock drift; (b) frequency responses of filter coefficients ($\mathbf{p}$ and $\mathbf{p}_{n,d}$).

where

$$\mathbf{p}^T = \frac{1}{M}\begin{bmatrix} 1 & 1 & \cdots & 1 \end{bmatrix}_{1 \times M},$$

$$\left(\mathbf{r}_n\right)^T = \begin{bmatrix} r(n,1) & r(n,2) & \cdots & r(n,M) \end{bmatrix}_{1 \times M}.$$

The transpose operation is represented by $(\cdot)^T$. The output of the symbol averaging is the same as the M-th filter output whose filter coefficient vector is $\mathbf{p}$. This filter is known as maximum ratio combining or matched filtering in communications, and it is optimal in white noise because it maximizes SNR of the output of the filter.

Assume that clock drift does not occur and the noise is uncorrelated temporally to examine the increment of SNR through the symbol averaging. Then the averaged chirp symbol is obtained as

$$r_{\text{avg}}(n) = \frac{1}{M}\sum_{m=1}^{M} r(n,m) = \frac{1}{M}\sum_{m=1}^{M}\left(x(n,m) + g(n,m)\right)$$

$$= x(n,1) + \frac{1}{M}\sum_{m=1}^{M} g(n,m) = x(n,1) + n(n). \qquad (5)$$

The noise variance on $r_{\text{avg}}(n)$ is given by $E[|n(n)|^2] = \sigma^2/M$. Therefore, SNR of $r_{\text{avg}}(n)$ is M times larger than that of $r(n,m)$.

In (5), the reason that multiple symbols can be simply averaged is that the symbols are coherent. However, when clock drift occurs, the multiple symbols are not coherent. Consequently, the compensating procedure of clock drift should be developed to add the multiple symbols coherently.

Figure 1 shows the symbol averaging in the frequency domain when the first samples of multiple chirp symbols are collected, for example. The samples $\mathbf{r}_n$ without clock drift are represented as solid line, and those $\mathbf{r}_{n,d}$ without clock drift are represented as dotted line. If there is no clock drift, $\mathbf{r}_n$ is a sync function with AWGN in the frequency domain. The filter coefficient vector $\mathbf{p}$ which is organized as all ones is employed to eliminate the noise. Then, the filter whose coefficients are $\mathbf{p}$ only cuts off the noise spectrum out of the spectrum of $\mathbf{r}_n$. Thus, the symbol averaging has an effect on the noise power reduction.

However, if clock drift exists, it causes CFO, sampling time offset, and symbol time offset. Then, the samples in $\mathbf{r}_n$ are distorted. As shown in Fig. 1, when the distorted samples are examined in the frequency domain, they are represented as the sync function with unknown phase shift which is described in section IV. So, the filter whose coefficient vector is $\mathbf{p}$ will cut off not only the noise spectrum but also the signal spectrum. To reduce the distortion of the clock drift and enhance SNR of the averaged symbol before TDE, the new coefficients $\mathbf{p}_{n,d}$ should be designed.

IV. Proposed SNR Enhancement Algorithm

To obtain filter coefficients, the relation between adjacent chirp symbols should be considered. To simplify the explanation, the noiseless chirp symbols are considered in this section. The effect of noise is demonstrated in section VI. Then, the received samples in (3) without AWGN are rearranged as

$$\tilde{r}(n,m) = \exp\left\{ j\left(m\left(\omega_{\text{CFO}}\left(T_{\text{sym}} - \kappa\right) + \frac{\pi\beta\kappa}{T_{\text{sym}}}\left(m\kappa - 2n\tilde{T}_s\right)\right) \right.\right.$$
$$\left. + n\tilde{T}_s\left(\frac{\pi\beta n\tilde{T}_s}{T_{\text{sym}}} + \omega_{\text{CFO}}\right) + \varphi \right)\right\}$$
$$\times \sqrt{E_s}\sum_{k=1}^{K}\alpha_k \exp\left(j\left(\frac{\pi\beta\tau_k}{T_{\text{sym}}}\left(\tau_k - 2n\tilde{T}_s + 2m\kappa\right)\right)\right),$$

$$\qquad (6)$$

where $(T_s - \varepsilon) = \tilde{T}_s$. It is safely assumed that $(mk - 2n\tilde{T}_s) = -2n\tilde{T}_s$ because of $\delta \ll (2n/(mN))$ in general. Thus, (6) can be approximated as

$$\tilde{r}(n,m) \approx \exp\left\{ j\left(m\left(\omega_{\text{CFO}}\left(T_{\text{sym}} - \kappa\right) - \frac{2\tilde{T}_s \pi\beta\kappa}{T_{\text{sym}}} n \right) \right.\right.$$
$$\left.\left. + n\tilde{T}_s\left(\frac{\pi\beta n\tilde{T}_s}{T_{\text{sym}}} + \omega_{\text{CFO}} \right) + \varphi \right) \right\}$$
$$\times \sqrt{E_s} \sum_{k=1}^{K} \alpha_k \exp\left(j\left(\frac{\pi\beta\tau_k}{T_{\text{sym}}}\left(\tau_k - 2n\tilde{T}_s \right) \right) \right). \quad (7)$$

Let $\omega_{\text{CFO}}(T_{\text{sym}} - \kappa)$ and $-(2\tilde{T}_s \pi\beta\kappa)/T_{\text{sym}}$ be ρ_1 and ρ_2, respectively. Without loss of generality, φ is set to zero. Then,

$$\tilde{r}(n,m) \approx z(n)\exp\left(jm\left(\rho_1 + n\rho_2 \right) \right), \quad (8)$$

where

$$z(n) = \exp\left(j\left(n\tilde{T}_s\left(\frac{\pi\beta n\tilde{T}_s}{T_{\text{sym}}} + \omega_{\text{CFO}} \right) + \varphi \right) \right)$$
$$\times \sqrt{E_s} \sum_{k=1}^{K} \alpha_k \exp\left(j\left(\frac{\pi\beta\tau_k}{T_{\text{sym}}}\left(\tau_k - 2n\tilde{T}_s \right) \right) \right).$$

In (8), the phase is linearly rotated by $\exp(j(\rho_1 + n\rho_2))$ as m increases for fixed n. Also, the phase is linearly rotated by $\exp(jm\rho_2)$ as n increases for fixed m. The proposed algorithm estimates the combined terms, ρ_1 and ρ_2, of CFO, sampling time offset, and symbol time offset. If ρ_1 and ρ_2 are estimated and compensated, all M chirp symbols will be identical to $z(n)$. Then, all M chirp symbols can be averaged to one chirp symbol by using symbol averaging because those are coherent. As a result, SNR of the averaged chirp symbol will be improved.

The key steps of the proposed SNR enhancement algorithm to estimate and compensate ρ_1 and ρ_2 and to increase SNR of the averaged chirp symbol are as follows:

Step 1. Multiply samples differentially at the same position between adjacent chirp symbols, and then add the multiplied results one another as

$$\tilde{r}_{\text{diff,sum}}(n) = \sum_{m=2}^{M}\left(\tilde{r}(n,m-1) \right)^* \tilde{r}(n,m)$$
$$= (M-1)\left| z(n) \right|^2 \exp\left(j\left(\rho_1 + n\rho_2 \right) \right). \quad (9)$$

Step 2. Multiply the adjacent multiplied results differentially as in (9), and then add the results one another as

$$\tilde{r}_{\text{total}} = \sum_{n=2}^{N}\left(\tilde{r}_{\text{diff,sum}}(n-1) \right)^* \tilde{r}_{\text{diff,sum}}(n)$$
$$= e^{j\rho_2}(M-1)^2 \sum_{n=2}^{N}\left| z(n-1) \right|^2 \left| z(n) \right|^2. \quad (10)$$

Step 3. Estimate ρ_2 by applying argument operation to (10) as

$$\hat{\rho}_2 = \arg\left(\tilde{r}_{\text{total}} / \left| \tilde{r}_{\text{total}} \right| \right), \quad (11)$$

where $\arg(\cdot)$ denotes argument operation and $|\cdot|$ denotes absolute value operation.

Step 4. Derotate $\tilde{r}_{\text{diff,sum}}(n)$ by multiplying $e^{-jn\hat{\rho}_2}$, add the results one another, and finally, estimate ρ_1 by applying argument operation as

$$\hat{\rho}_1 = \arg\left(\sum_{n=1}^{N}\tilde{r}_{\text{diff,sum}}(n)\exp\left(-jn\hat{\rho}_2 \right) \middle/ \left| \sum_{n=1}^{N}\tilde{r}_{\text{diff,sum}}(n)\exp\left(-jn\hat{\rho}_2 \right) \right| \right).$$
$$(12)$$

Step 5. Generate the filter coefficients based on the estimated ρ_1 and ρ_2 as

$$p(n,m) = \exp\left(-j\left(m\left(\hat{\rho}_1 + n\hat{\rho}_2 \right) \right) \right). \quad (13)$$

Then, filter the received samples by $p(n,m)$ as follows:

$$\tilde{r}_{\text{avg}}(n) = \sum_{m=1}^{M} p(n,m)\tilde{r}(n,m)$$
$$= \left(\sum_{m=1}^{M} z(n)e^{jm(\rho_1 + n\rho_2)}e^{-jm(\hat{\rho}_1 + n\hat{\rho}_2)} \middle/ M \right) = \left(\sum_{m=1}^{M} z(n) \middle/ M \right)$$
$$= \sqrt{E_s} \sum_{k=1}^{K} \alpha_k \exp\left(j\left(nT_s\left(\frac{\pi\beta nT_s}{T_{\text{sym}}} - \frac{2\pi\beta}{T_{\text{sym}}}\left(n\varepsilon + \tau_k \right) + \omega_{\text{CFO}} \right) \right.\right.$$
$$\left.\left. + \frac{\pi\beta}{T_{\text{sym}}}\left(n\varepsilon + \tau_k \right)^2 - \omega_{\text{CFO}} n\varepsilon \right) \right).$$
$$(14)$$

In (14), the perfect estimation of ρ_1 and ρ_2 is assumed. The new filter coefficient vector $\mathbf{p}_{n,d}$ of the proposed algorithm as shown in Fig. 1 is

$$\mathbf{p}_{n,d} = \frac{1}{M}\left[p(n,1) \quad p(n,2) \quad \cdots \quad p(n,M) \right]^T. \quad (15)$$

Consequently, the phase distortion induced by CFO, sampling time offset, and symbol time offset is reduced through the filtering operation; simultaneously, SNR of the averaged chirp symbol is enhanced. The averaged chirp symbol in (14) can be approximated as in (16) because of $\varepsilon \approx \delta T_s$.

$$\tilde{r}_{\text{avg}}(n) \approx \tilde{r}_{\text{avg,appr}}(n)$$
$$= \sqrt{E_s} \sum_{k=1}^{K} \alpha_k \exp\left(j\left(nT_s\left(\frac{\pi\beta nT_s}{T_{\text{sym}}} - \frac{2\pi\beta}{T_{\text{sym}}}\tau_k + \omega_{\text{CFO}} \right) \right.\right.$$
$$\left.\left. + \frac{\pi\beta}{T_{\text{sym}}}\left(\tau_k \right)^2 \right) \right).$$
$$(16)$$

V. Time Delay Estimation Using the Averaged Chirp Symbol

Although ρ_1 and ρ_2 are estimated and compensated by using the proposed algorithm, CFO still remains as in (16). The ω_{CFO}

can be eliminated by using the relationship between up-chirp and down-chirp after TDE is performed as in (19).

The dechirping process is performed as in [2], which multiplies $\tilde{r}_{\text{avg,appr}}(n)$ by the conjugate of $s(n)$ as

$$
\begin{aligned}
&\tilde{r}_{\text{avg,appr}}(n)s^{*}(n) \\
&= \sqrt{E_s}\sum_{k=1}^{K}\alpha_k \exp\left(j\left(nT_s\left(-\frac{2\pi\beta}{T_{\text{sym}}}\tau_k+\omega_{\text{CFO}}\right)+\frac{\pi\beta}{T_{\text{sym}}}(\tau_k)^2\right)\right)
\end{aligned}
\tag{17}
$$

to apply the averaged chirp symbol to the frequency estimation algorithm based on the subspace separation in [3]. Then, the time delay of the first arrival path is estimated as

$$
\hat{\theta}=T_s\left(-\frac{2\pi\beta}{T_{\text{sym}}}\tau_1+\omega_{\text{CFO}}\right) \Rightarrow \tau_1=-\frac{T_{\text{sym}}}{2\pi\beta T_s}\hat{\theta}+\frac{T_{\text{sym}}}{2\pi\beta}\omega_{\text{CFO}},
\tag{18}
$$

where $\hat{\theta}$ denotes the estimated phase between adjacent samples of (17) through the frequency estimation algorithm.

Because the TDE results obtained from the up-chirp and the down-chirp have the opposite sign except the term having ω_{CFO} due to the relationship between up-chirp and down-chirp, the time delay of the first arrival path unaffected by CFO is obtained by subtracting the TDE result of the up-chirp from that of the down-chirp as

$$
\begin{aligned}
\tau_1 &= \frac{1}{2}\left(\frac{T_{\text{sym}}}{2\pi\beta T_s}\hat{\theta}+\frac{T_{\text{sym}}}{2\pi\beta}\omega_{\text{CFO}}-\left(-\frac{T_{\text{sym}}}{2\pi\beta T_s}\hat{\theta}+\frac{T_{\text{sym}}}{2\pi\beta}\omega_{\text{CFO}}\right)\right) \\
&= \frac{T_{\text{sym}}}{2\pi\beta T_s}\hat{\theta}.
\end{aligned}
\tag{19}
$$

VI. Mathematical Analysis

In this section, the proposed algorithm is mathematically analyzed in a multipath channel with AWGN, and the amount of SNR enhancement is described after applying the proposed algorithm. In [11], provided that SNR is sufficiently high, a signal A with AWGN can be approximated as

$$
A+N_R+jN_I \approx Ae^{j\eta},
\tag{20}
$$

where N_R and N_I are independent zero mean Gaussian random variables with variance σ^2, and η is phase noise. According to [12], the probability distribution function of η can be approximated as a Gaussian distribution with $\sigma^2/2$. Then, the received chirp samples corrupted by multipath channel with AWGN can be approximated as

$$
r(n,m)\approx z(n)e^{jm(\rho_1+n\rho_2)}+g(n,m)\approx z(n)e^{jm(\rho_1+n\rho_2)}e^{j\psi(n,m)},
\tag{21}
$$

where the phase noise $\psi(n,m)$ induced by AWGN denotes

the uncorrelated and zero-mean Gaussian variables with $\sigma^2/2$ as in [11]. The proposed algorithm deals only with the phase terms; therefore, the approximation in (21) is valid. Based on (21), (9) is restated as

$$
\begin{aligned}
r_{\text{diff,sum}}(n) &= |z(n)|^2 e^{j(\rho_1+n\rho_2)}\sum_{m=2}^{M}e^{-j\psi(n,m-1)}e^{j\psi(n,m)} \\
&\approx e^{j(\rho_1+n\rho_2)}|z(n)|^2(M-1)e^{j\left(\frac{\psi(n,M)-\psi(n,1)}{M}\right)}.
\end{aligned}
\tag{22}
$$

After that, (10) can be expressed as

$$
\begin{aligned}
r_{\text{total}} &\approx (M-1)^2(N-1)e^{j\left(\rho_2+\frac{\psi(N,M)-\psi(N,1)-\psi(1,M)+\psi(1,1)}{(M-1)(N-1)}\right)} \\
&\times \sum_{n=2}^{N}|z(n-1)|^2|z(n)|^2.
\end{aligned}
\tag{23}
$$

Then,

$$
\begin{aligned}
\hat{\rho}_2 &= \arg\left(r_{\text{total}}/|r_{\text{total}}|\right)=\rho_2+\varepsilon_2 \\
&= \rho_2+\frac{\psi(N,M)-\psi(N,1)-\psi(1,M)+\psi(1,1)}{(M-1)(N-1)}.
\end{aligned}
\tag{24}
$$

The error term, which is the second term in (24), is denoted as ε_2. To estimate ρ_1, $r_{\text{diff,sum}}(n)$ is derotated by using the estimated ρ_2 as

$$
\begin{aligned}
&r_{\text{diff,sum,der}}(n)=\sum_{n=1}^{N}r_{\text{diff,sum}}(n)\exp(-jn\hat{\rho}_2) \\
&\approx N(M-1)e^{j\left(\rho_1+\left(\left[\frac{1}{N(M-1)}\sum_{n=1}^{N}(\psi(n,M)-\psi(n,1))\right]-\left[\frac{\psi(N,M)-\psi(N,1)-\psi(1,M)+\psi(1,1)}{2(M-1)}\right]\right)\right)}\sum_{n=1}^{N}|z(n)|^2.
\end{aligned}
\tag{25}
$$

The estimated ρ_1 can be obtained as

$$
\begin{aligned}
\hat{\rho}_1 &= \arg\left(r_{\text{diff,sum,der}}(n)/|r_{\text{diff,sum,der}}(n)|\right)=\rho_1+\varepsilon_1 \\
&= \rho_1+\left(\left(\frac{1}{N(M-1)}\sum_{n=1}^{N}(\psi(n,M)-\psi(n,1))\right)\right. \\
&\left.-\left(\frac{\psi(N,M)-\psi(N,1)-\psi(1,M)+\psi(1,1)}{2(M-1)}\right)\right).
\end{aligned}
\tag{26}
$$

The error term, which is the second term in (26), is also denoted as ε_1. Then, multiple chirp symbols are added after eliminating ρ_1 and ρ_2 as

$$
\begin{aligned}
r_{\text{avg}}(n) &= \sum_{m=1}^{M}z(n)e^{jm(\rho_1+n\rho_2)}e^{j\psi(n,m)}e^{-jm(\hat{\rho}_1+n\hat{\rho}_2)} \\
&= \sum_{m=1}^{M}z(n)e^{j(\psi(n,m)-m(\varepsilon_1+n\varepsilon_2))} \\
&\approx z(n)\sum_{m=1}^{M}\left(1+j\left(\psi(n,m)-m(\varepsilon_1+n\varepsilon_2)\right)\right).
\end{aligned}
\tag{27}
$$

The expected value of $r_{\text{avg}}(n)$ is

$$E\left[r_{\text{avg}}(n)\right] = \frac{M(M-1)}{2}z(n). \qquad (28)$$

Also, the variance is

$$\text{var}\left[r_{\text{avg}}(n)\right] = \left(z(n)\right)^2 \left\{ M\sigma_\psi^2 + \left(M(M-1)/2\right)^2 E\left[\left(\varepsilon_1 + n\varepsilon_2\right)^2\right] \right.$$
$$- M(M-1)E\left[\varepsilon_1\left(\sum_{m=1}^{M}\psi(n,m)\right)\right]$$
$$\left. - M(M-1)E\left[n\varepsilon_2\left(\sum_{m=1}^{M}\psi(n,m)\right)\right]\right\},$$

$$(29)$$

where

$$E[\varepsilon_1] = E[\varepsilon_2] = 0, \; E[\varepsilon_1^2] = \frac{(N-2)\sigma_\psi^2}{2N(M-1)},$$

$$E[\varepsilon_2^2] = \frac{2\sigma_\psi^2}{(M-1)^2(N-1)^2},$$

$$E[\varepsilon_1\varepsilon_2] = \frac{\sigma_\psi^2}{2N(N-1)(M-1)^2}\left(\frac{1}{N} - \frac{1}{2}\right).$$

Note that σ_ψ^2 denotes the variance of $\psi(n,m)$. By using the approximation equation of SNR as in [13], the amount of SNR enhancement can be derived as

$$SNR_{\text{enhancement}} \approx \frac{\left(E\left[r_{\text{avg}}(n)\right]\right)^2}{\text{var}\left[r_{\text{avg}}(n)\right]}$$

$$= \frac{8MN(N-1)^2}{\sigma_\psi^2\left(4N(N-1)^2 + M(N+2)(N-1)^2 - 4nMN(N-1) + 4n^2MN\right)}. \qquad (30)$$

VII. Simulation Results

In this section, simulation results are provided to verify the amount of SNR enhancement and to study the performance improvement of TDE after implementing the proposed algorithm. For simulations, the chirp signal of IEEE 802.15.4a in [14] is used. The chirp signal in IEEE 802.15.4a is composed of up-chirp signal and down-chirp signal. Simulation results are obtained over 10,000 realizations. System parameters used in the simulations are β=6.3 MHz, T_s=1/32 μs, and T_{sym}=1.1875 μs as in [14]. The center frequency ω_c is 2.4 GHz. In all simulations, the clock offset δ is set to the maximum clock offset as in [14], that is, 80 ppm. The ESPRIT algorithm is chosen as a TDE algorithm because of its simplicity and good estimation performance. The simulations are conducted with the Saleh-Valenzuela (SV) model, which is
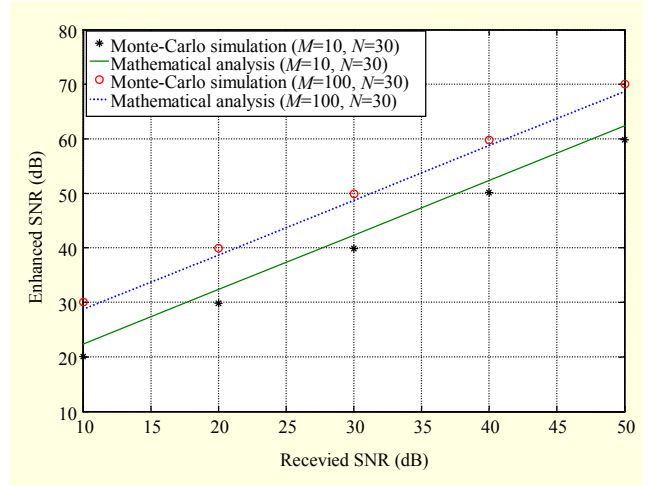

Fig. 2. Enhanced SNR of proposed algorithm versus received SNR (different number of symbol averaging: M=10 and M=100).
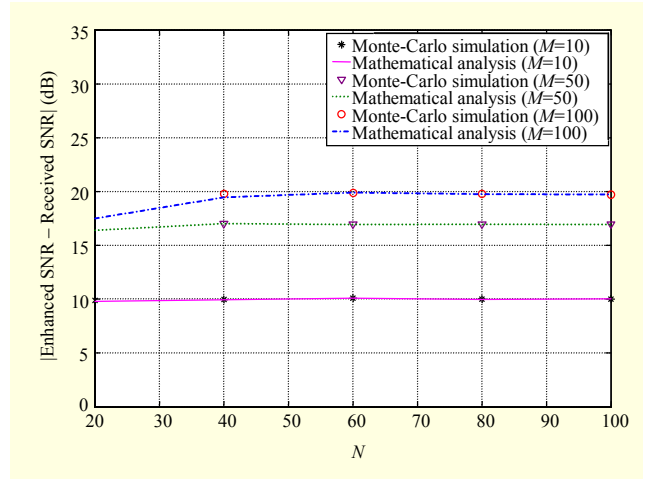

Fig. 3. Difference between enhanced SNR and received SNR versus number of samples in a symbol (M=10, M=50, and M=100).

a statistical indoor channel model that reflects that multipath arriving in measured channels in clusters in [15]. In the SV model, the power delay profile contains a number of clusters, and each cluster contains a number of ray paths. Four multipath channels are employed: CM1 (residential line of sight (LOS)), CM2 (residential nonline of sight (NLOS)), CM3 (office LOS), and CM4 (office NLOS).

Figure 2 shows the simulation results for the proposed SNR enhancement algorithm. In this figure, we plotted enhanced SNR versus received SNR when M is varied. Enhanced SNR denotes SNR of the averaged chirp symbol obtained from the proposed SNR enhancement algorithm. Analytical enhanced SNR is represented as $SNR_{\text{enhancement}}$ in (30). Received SNR is defined as E_s in (2), that is, energy of the received signal. By
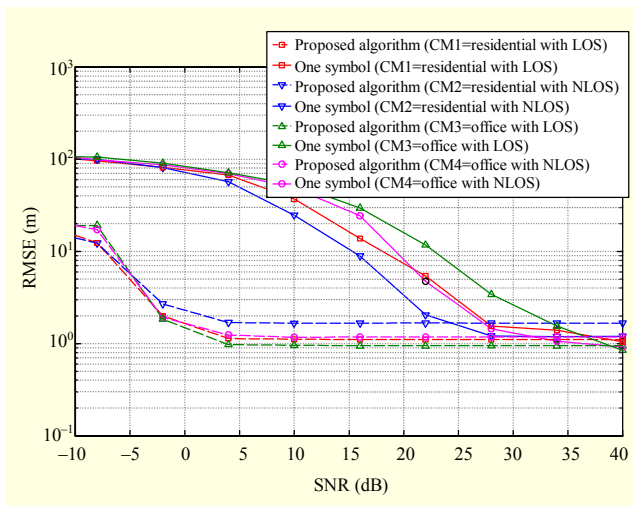
Fig. 4. RMSE of ESPRIT algorithm by using averaged chirp (M=100, N=30) and single chirp (M=1, N=30).

comparing Monte-Carlo simulation results for different M, the increment of M shows the increment of SNR of the averaged chirp symbol because the proposed algorithm converts the increment of the number of chirp symbols into the increment of SNR. Also, Monte-Carlo simulation agrees with the mathematical analysis. Therefore, the approximation (20) that we assumed in section VI is verified to be reasonable.

Figure 3 shows the difference between enhanced SNR and received SNR versus the number of samples. Difference between SNRs increases as M increases, whereas that between SNRs has little change as N increases. The increment of M indicates the increment of the number of chirp symbols; however, that of N does not cause that of the number of chirp symbols.

In Fig. 4, the root mean square error (RMSE) of the TDE versus the SNR is plotted for 80 ppm clock offset in multipath channel. One symbol denotes the situation where the proposed algorithm is not employed before TDE. When CFO, sampling time offset, and symbol time offset are not compensated, high SNR (more than 25 dB) is necessary in order to reach the RMSE within 2 meters. However, at most, 5 dB is needed when the proposed algorithm is employed. The TDE performance is improved regardless of the existence of LOS. Moreover, all RMSEs are saturated because the number of samples and the bandwidth are deficient to resolve all ray paths (> 100) in multipath channel.

VIII. Conclusion

An SNR enhancement algorithm is proposed to improve the accuracy of the positioning system using multiple chirp symbols in the environment with severe clock drift. The combined terms of CFO, sampling time offset, and symbol time offset are eliminated in consideration of the linear phases between multiple chirp symbols. Moreover, the effect of extension of observation time based on multiple chirp symbols is converted into that of the increment of SNR. Simulation results show that more than $10\log_{10}M$ dB SNR gain is obtained when M chirp symbols distorted by clock drift are employed. In conclusion, the performance of TDE using the averaged chirp symbol is improved as the number of chirp symbols increases.

References

[1] G.W. Deley, "Waveform Design," *Radar Handbook*, M.I. Skolnik, Ed., 1st ed., New York: McGraw-Hill, 1970.

[2] S.H. Jang et al., "Performance Optimization of Time Delay Estimation Based on Chirp Spread Spectrum Using ESPRIT," *IEICE Trans. Commun.*, vol. E94-B, no. 2, Feb. 2011, pp. 607-609.

[3] R. Roy and T. Kailath, "ESPRIT-Estimation of Signal Parameters via Rotational Invariance Techniques," *IEEE Trans. Acoustics, Speech, Signal Process.*, vol. 37, no. 7, July 1989, pp. 984-995.

[4] S. Gezici et al., "Localization via Ultra-wideband Radios: A Look at Positioning Aspects for Future Sensor Networks," *IEEE Signal Process. Mag.*, vol. 22, no. 4, July 2005, pp. 70-84.

[5] L. Wu et al., "A Closed-Form Blind CFO Estimator Based on Frequency Analysis for OFDM Systems," *IEEE Trans. Commun.*, vol. 57, no. 6, June 2009, pp. 1634-1637.

[6] K.-C. Hung and D.W. Lin, "Pilot-Aided Multicarrier Channel Estimation via MMSE Linear Phase-Shifted Polynomial Interpolation," *IEEE Trans. Wireless Commun.*, vol. 9, no. 8, Aug. 2010, pp. 2539-2549.

[7] Y. Saito and Y. Sanada, "Effect of Clock Offset on an Impulse Radio Ultra Wideband Ranging System with Comparators," *IET Commun.*, vol. 3, no. 6, June 2009, pp. 1024-1029.

[8] B. Zhen, H.-B. Li, and R. Kohno, "Clock Management in Ultra-wideband Ranging," *16th IST Mobile Wireless Commun.*, July 2007, pp. 1-5.

[9] R. Hach, "Symmetric Double Side Two Way Ranging," IEEE 802.15 WPAN documents, 15-05-0334-r00.

[10] D.G. Oh, S.H. Yoon, and J.W. Chong, "A New Subspace-Based Time Delay Estimation of Chirp Spread Spectrum," *IEICE Trans. Commun.*, vol. E92-B, no. 4, Apr. 2009, pp. 1418-1421.

[11] H. Leib and S. Pasupathy, "The Phase of a Vector Perturbed by Gaussian Noise and Differentially Coherent Receivers," *IEEE Trans. Info. Theory*, vol. 34, no. 6, Nov. 1988, pp. 1491-1501.

[12] F. Adachi and M. Sawahashi, "Decision Feedback Differential Phase Detection of M-ary DPSK Signals," *IEEE Trans. Vehicular Technol.*, vol. 44, no. 2, May 1995, pp. 203-210.

[13] T.M. Schmidl and D.C. Cox, "Robust Frequency and Timing

Synchronization for OFDM," *IEEE Trans. Commun.*, vol. 45, no. 12, Dec. 1997, pp. 1613-1621.

[14] IEEE 802.15.4a-2007, "Part 15.4: Wireless Medium Access Control (MAC) and Physical Layer (PHY) Specifications for Low-Rate Wireless Personal Area Networks (WPANs); Amendment 1: Add Alternate PHYs," Mar. 2007.

[15] A.F. Molisch et al., "IEEE 802.15.4a Channel Model–Final Report," IEEE 802.15-04-0662-00-004a, San Antonio, TX, USA, Nov. 2004.

Seong-Hyun Jang received the BS in electronic and computer engineering from Hanyang University, Seoul, Rep. of Korea, in 2006. Since 2006, he has been a research assistant at the Department of Electronic and Computer Engineering, Hanyang University, where he is currently working toward his PhD degree. His research interests include localization systems, synchronization, and its VLSI implementation.

Yeong-Sam Kim received the BS, MS, and PhD in electronic and computer engineering from Hanyang University, Seoul, Rep. of Korea, in 2005, 2007, and 2011, respectively. His research interests include localization and modem algorithms for WPAN and its VLSI implementation.

Sang-Hun Yoon received the PhD from Hanyang University, Seoul, Rep. of Korea, in 2008. Since 2009, he has worked for ETRI, Daejeon, Rep. of Korea, where he is currently a senior member of the engineering staff. His research areas include ASIC design, digital signal processing, wireless communication system design, and image processing.

Jong-Wha Chong received his BS and MS in electronics engineering from Hanyang University, Seoul, Rep. of Korea, in 1975 and 1979, respectively. He received his PhD in electronics and communication engineering from Waseda University, Japan, in 1981. From 1979 to 1980, he was a researcher in the C&C research center of Nippon Electronic Company (NEC). From 1983 to 1984, he was a researcher at the Korean Institute of Electronics & Technology (KIET). From 1986 to 1987, he was a visiting professor at the University of California, Berkeley, USA. From 1993 to 1994, he served as chairperson of the CAD & VLSI Society at the Institute of the Electronic Engineers of KOREA (IEEK). From 1995 to 1997, he was a visiting professor at the University of Newcastle Upon-Tyne, England, and from 1997 to 1999, he was the Dean of the Information and Communication Center, Hanyang University. He has been a professor of the Department of Electronics Engineering, Hanyang University, Seoul, Rep. of Korea since 1981, and has been the vice chairman of the IEEK since 2002. His current research interests are the design of ASIC emulation systems, CAD for VLSI, H.264 encoder/decoder design, JPEG2000 encoder design, and communication circuit design, particularly in UWB modem design.